RSC Advances

PAPER

View Article Online
View Journal | View Issue

Cite this: *RSC Adv.*, 2018, **8**, 11921

Photocatalytic degradation of rhodamine B catalyzed by TiO_2 films on a capillary column

Huaitao Yang and Junjiao Yang *

Received 17th January 2018
Accepted 13th March 2018

DOI: 10.1039/c8ra00471d

rsc.li/rsc-advances

TiO_2 films on a capillary column were prepared using tetrabutoxytitanium as a source of TiO_2 *via* the sol–gel method. The film thickness showed a linear increase with tetrabutoxytitanium concentration. The specific surface area of the film was improved by adding polyethylene glycol with different molecular weights. Under optimal conditions, the prepared film had a good mesoporous structure with specific surface area of 47.72 m^2 g^{-1}, and showed nearly spherical nanoparticles with a 10 nm diameter and anatase phase. Influences of the thickness, specific surface area, and initial solution concentration on photodegradation of rhodamine B using TiO_2 films as a catalyst were investigated. The results showed that the photodegradation efficiency increased with an increasing thickness and specific surface area of TiO_2 films. For a rhodamine B solution of 15 mg L^{-1}, the photodegradation efficiency was 98.33% in 30 min under the optimal conditions. The catalysts could be reused up to eight times with almost the same efficiency, indicating a firm immobilization of films on the inner wall of the capillary. Therefore, TiO_2 films are promising for the treatment of wastewater.

1 Introduction

Global industrialization is ever developing but at the same time, the environmental pollution is ever worsening. Especially, organic pollutants in water cannot be completely removed by traditional water treatment technologies. Photocatalysis may overcome this problem as it directly uses solar energy to drive the reaction, and is an ideal environmental pollution purification technology.[1] The semiconductor TiO_2 is an important photocatalyst and has been widely employed in photodegradation of organic pollutants,[2,3] solar cells,[4] gas sensors,[5] and hydrogen production by water splitting.[6]

In recent years, many researchers have studied photocatalysis using powder[7,8] or thin film[9–11] titania. Powder titania has a wider application because of its high specific surface area, quantum yield, and photocatalytic efficiency. However, powder titania cannot be recycled and the resulting high treatment cost limits its application in industry. Thus, there has been an increasing interest in the preparation of films of titania to solve this problem. Considering the fragility of films, large mechanical strength substrates with strong physical or chemical bond between the film and the body are needed. The substrates can be classified as metal,[12,13] glass,[14,15] ceramic[16] and so on. Traditionally, titania was supported on these substrates by a physical technique, which has some drawbacks like film shedding and difficulty in recycling of the film. Thus, further study is needed on high efficiency photocatalytic reactors.

In this paper, we described the utility of the quartz capillary with hydroxyl silicon on the inner wall as the substrate for TiO_2 films and their application for photodegradation of rhodamine B. Through a sol–gel method,[17,18] TiO_2 films were deposited on the inner wall of the capillary based on the condensation reaction between hydroxyl silicon and hydroxy titanium. Such films can be firmly immobilized on the capillary inner wall by chemical bond that can effectively prevent the films from the substrate falling off.[19,20] Additionally, the sol–gel method has the advantages of low cost and simple operation compared with spin coating,[21] LbL technique[22,23] and magnetron sputtering.[24] In our research, a sustainable and cost-effective approach of adequately removing the contaminants from wastewater was found. Furthermore, catalyst reusability study has also been conducted to prove that the method is very earthshaking for both economy and environment.

2 Experimental section

2.1 Materials

Fused-silica capillaries with 500 μm I.D. were purchased from Yongnian Fiber Plant (Hebei, China). Tetrabutoxytitanium (TBOT), acetic acid (HAc), ethanol (EtOH), poly ethylene glycol (PEG), sodium hydroxide (NaOH), and rhodamine B (RhB).

2.2 Preparation of TiO_2 films on capillary column

2.2.1 Capillary pretreatment. The fused silica capillaries of a certain length were injected with 1 mol L^{-1} NaOH by a syringe,

Beijing Key Laboratory of Environmentally Harmful Chemical Analysis, Beijing University of Chemical Technology, Beijing 100029, China. E-mail: yangjj@mail.buct.edu.cn; Tel: +86 13691589336

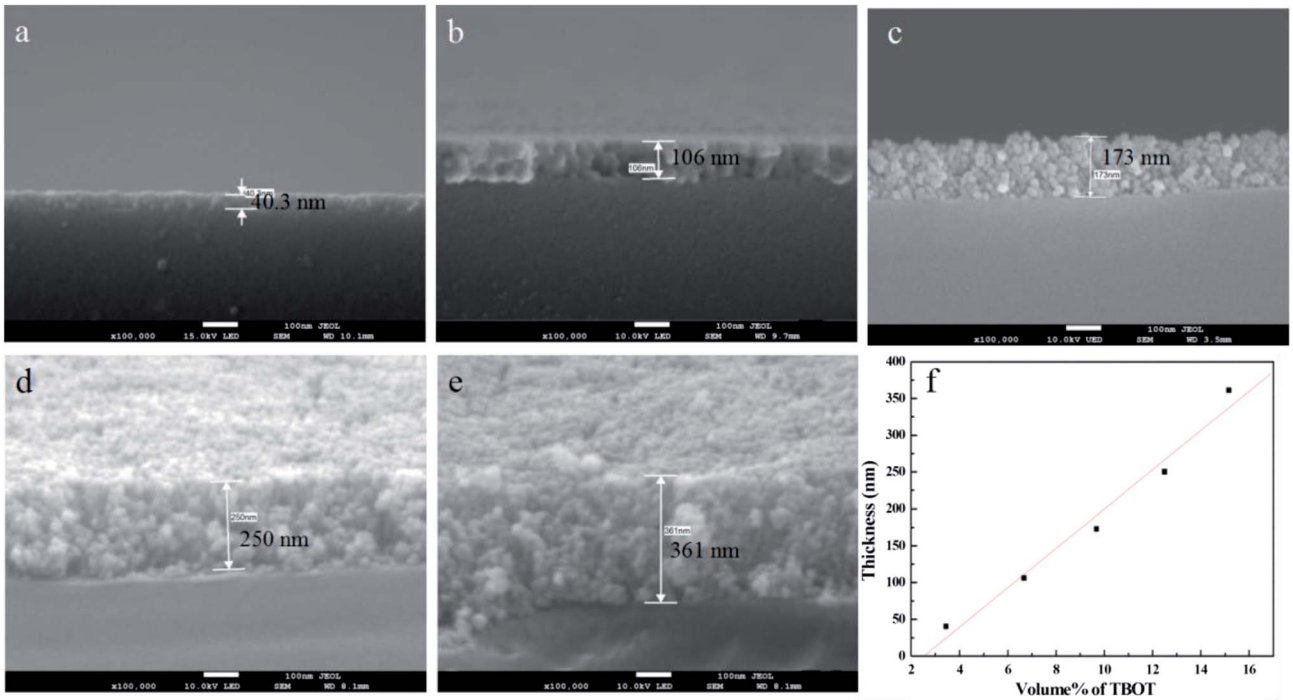

Fig. 1 Cross-sectional SEM images of TiO_2 films when the percentage volume of TBOT is (a) 3.45%, (b) 6.67%, (c) 9.68%, (d) 12.5%, and (e) 15.15%. (f) Linear relationship of thickness with the concentration of TBOT.

followed by sealing at both ends with silicone rubber and putting them in a 60 °C water bath to activate the silanol groups on the capillaries wall for 2 h. Then capillaries were rinsed with water (25 °C) and absolute ethanol (25 °C), followed by drying in the oven (120 °C) for 2 h to remove the ethanol.

2.2.2 Catalyst preparation. The titania sols were prepared from a solution containing tetrabutoxytitanium, ethanol, acetic acid, deionized water and poly ethylene glycol. In a typical synthesis procedure, 10 ml of ethanol, a certain amount of TBOT (in this experience, the volume content of TBOT is 3.45%, 6.67%, 9.68%, 12.5% and 15.15%) and 4 ml of acetic acid were mixed in a 50 ml small beaker labeled as "A". Subsequently, 10 ml of ethanol, 2 ml of deionized water and 2 ml of PEG were added into another beaker labeled as "B", and then put them into 0–5 °C ice-water bath. The solution A was added dropwise into the solution B with magnetic stirring for 20 min to form a homogeneous and transparent precursor solution which was then injected into the pretreated capillaries. After being sealed at both end, the capillaries continued to further be kept at 50 °C (water bath) for 6 h and then dried at 120 °C for 3 h in oven. Then, the capillaries were washed with ethanol and water to remove residual compounds, and later dried under room temperature. Finally, the prepared capillary column was placed into a muffle furnace heating up to 500 °C at a rate of 5 °C min^{-1}

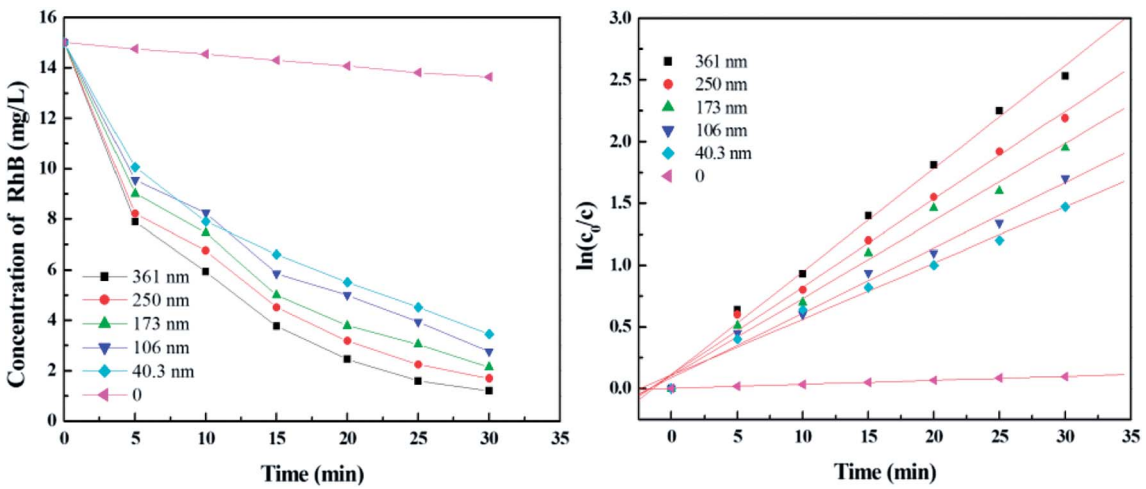

Fig. 2 Photodegradation of RB under UV irradiation by films with different thickness.

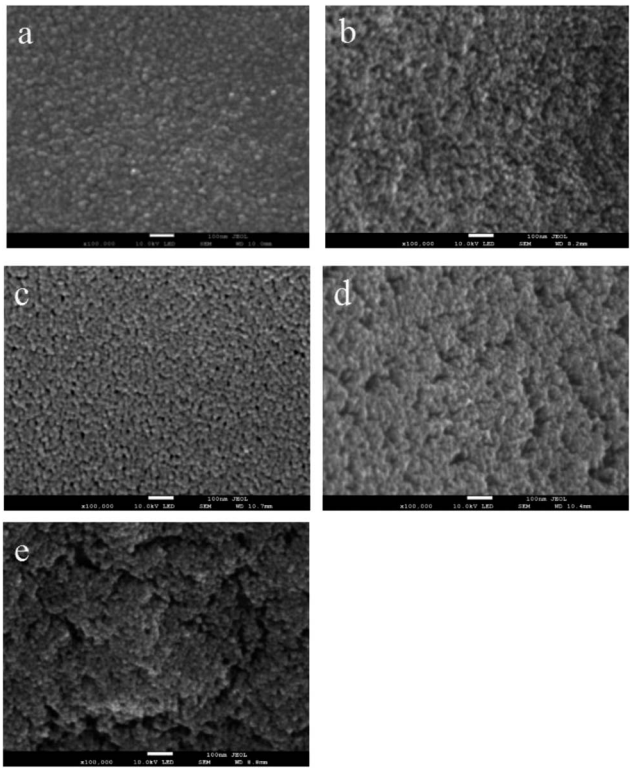

Fig. 3 SEM images of TiO_2 films with PEG of different molecular weight: (a) PEG 400, (b) PEG 800, (c) PEG 1000, (d) PEG 1500, and (e) PEG 2000.

to calcine for 5 h. Consequently, anatase TiO_2 was formed, and at the same time the organic compounds were completely removed. This approach is facile, and we could accomplish the whole procedure within one day.

2.3 Photodegradation experiments

The photodegradation experiments were conducted with rhodamine B injected into the capillaries deposited by TiO_2 films. The capillaries were placed in a distance of 10 cm away from the UV lamp of 5 W. All photodegradation experiments were conducted with 15 mg L^{-1} rhodamine B at room temperature in air unless or otherwise mentioned.

2.4 Characterization

Scanning electron microscopy (SEM) images were obtained on a JEOL JSM-7800F scanning electron microscope. The film thickness was determined from its cross-sectional SEM image. Powder X-ray diffraction (XRD) data were collected on a Shimadzu Model XRD-6000 powder diffractometer, using Cu Kα radiation (30 mA and 40 kV) in the 2θ range of 20–70°, with a scanning rate of 10° min^{-1}. Nitrogen adsorption–desorption isotherms (SSA-6000E, Micromeritics Instruments) were collected at 77 K. High resolution transmission electron microscopy (HRTEM) observations were carried out on JEOL JEM-ARM200F atomic resolution analytical microscope operated at 200.0 kV. The photodegradation of RB was analyzed using Shimadzu LC-6A high performance liquid chromatography and Waters Quattro Premier XE ultra high performance liquid chromatography-mass spectrometry (UPLC-MS).

3 Results and discussion

3.1 Titanium source content of TiO_2 films

3.1.1 Thickness of TiO_2 films. To develop a moderate and controllable system, we introduced acetic acid and ethanol to slow down the hydrolysis rate of tetrabutoxytitanium. The CH_3COO^- from HAc as a coordination group can replace *n*-butoxy of $Ti(OBu^n)_4$ to form $Ti(OBu^n)_{4-x}(CH_3COO)_x$ complex, whose reaction rate toward water is slower than that of $Ti(OBu^n)_4$. As a result, acetic acid can effectively prevent the surface Ti species from further hydrolysis and condensation *via* the coordination. On the other hand, H^+ from acetic acid adsorbed on the particles surface could form the electric double layer and inhibit the interaction between titanium hydroxyl groups. This mechanism has been comprehensively discussed in the previous studies.[25–27] Thus, acetic acid in the system does well in controlling the hydrolysis and condensation of tetrabutoxytitanium. To obtain a smooth and compact film, a certain amount of PEG was added into the mixture to prevent cracks by reducing the surface tension between the titania particles and increase specific surface area.

The growth of TiO_2 films on the capillary was controlled by changing the amount of TBOT. Fig. 1 shows the corresponding cross-sectional SEM images of TiO_2 films with thickness of 40.3 nm, 106 nm, 173 nm, 250 nm and 361 nm when the percentage volume of TBOT is 3.45%, 6.67%, 9.68%, 12.5% and 15.15%, respectively. As shown in Fig. 1, the thickness increases linearly with the concentration of TBOT increased, probably because the more TBOT is available, the more load films have. As revealed by SEM images, the films possess a smooth and compact surface layer with nanoparticles, and the framework adheres tightly to the inner wall of capillary, suggesting a good anchorage. However, if the percentage volume of TBOT exceeds 15.15%, the reaction would be difficult to control, leading to a rapid formation of white precipitates instead of precursor solution. As a consequence, we acquired a maximum thickness of 361 nm for TiO_2 films in the presence of 15.15% TBOT in our research.

3.1.2 Photodegradation reaction of rhodamine B. To compare the degradation efficiency of the immobilized films with different thickness, photodegradation experiments were conducted with rhodamine B injected into the capillaries that deposited by multiple thicknesses of films. As shown in Fig. 2, the degradation efficiency increases from 77% to 92.07% with thickness from 40.3 nm to 361 nm in 30 min. The photodegradation rate constants calculated from the corresponding kinetic curves are 0.0455, 0.0527, 0.0628, 0.0711 and 0.0835 min^{-1}, for the thickness of 40.3, 106, 173, 250, and 361 nm, respectively, indicating that the degradation rate increases as the thickness of films increases. The reason might be that the availability of more catalysts results in a better degradation efficiency. For comparison, a control experiment was carried out using the naked capillary filled with rhodamine

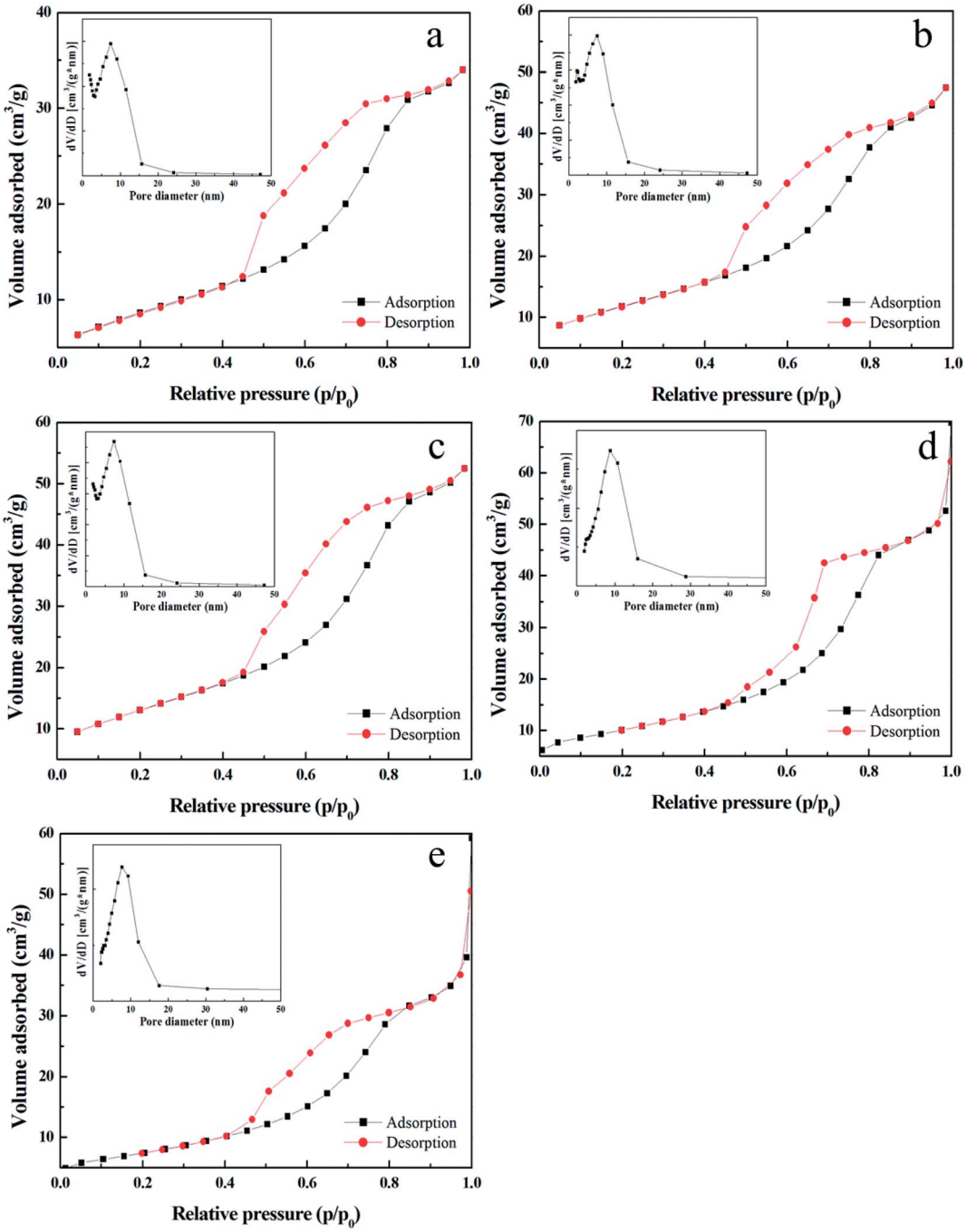

Fig. 4 Nitrogen adsorption–desorption isotherms and the pore size distribution curves (inset) for TiO_2 films with (a) PEG 400, (b) PEG 800, (c) PEG 1000, (d) PEG 1500, and (e) PEG 2000.

B. The result shows that almost no RB was degraded in this case, confirming that the high efficiency of RB degradation comes from the catalysts instead of UV irradiation.

3.2 PEG molecular weight of TiO_2 films

3.2.1 Morphological and structural characterization of films. The polyethylene glycol with large molecular weight can occupy a certain space on TiO_2 film, resulting in a pore on the surface after calcination at high temperature. Therefore, PEGs with different molecular weight were added to increase the specific surface area of film, and films were deposited using TBOT with percentage volume of 15.15%. Fig. 3 presents the SEM images of TiO_2 film with PEG of molecular weight of 400, 800, 1000, 1500, and 2000. It can be seen that when the molecular weight of PEG is more than 1000, cracks appear on the film surface because of its phase separation in ethanol solution. Fig. 4 shows the corresponding nitrogen adsorption–desorption isotherms and pore size distribution curves of the

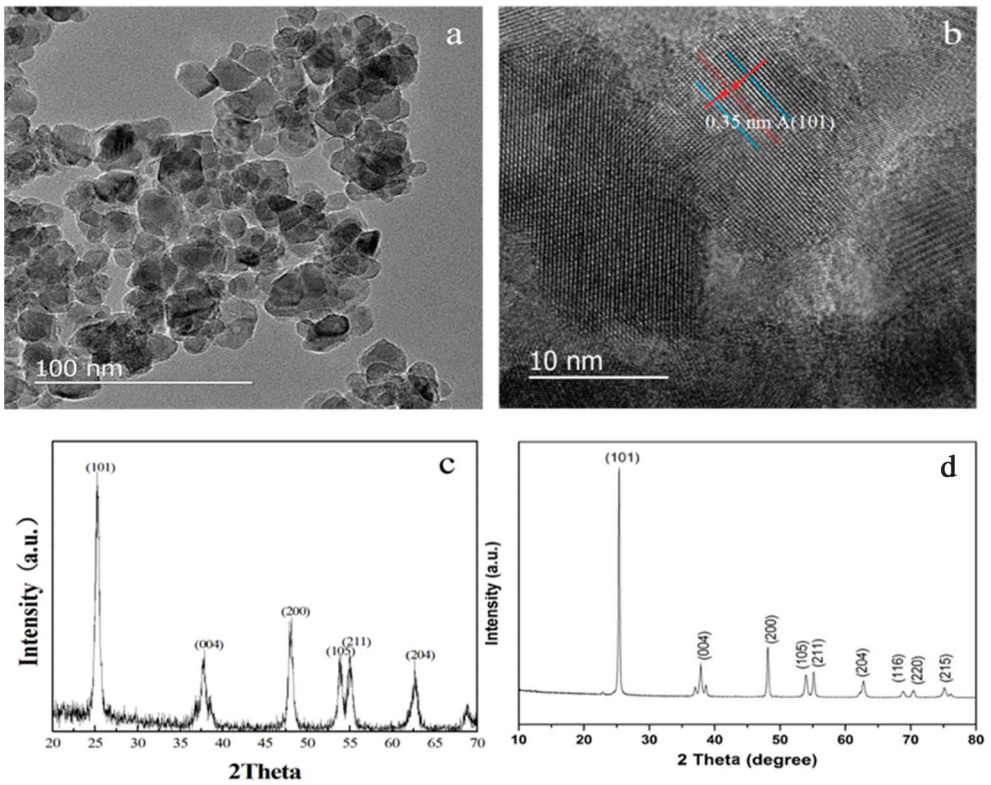

Fig. 5 HRTEM images (a and b) and XRD (c) pattern of catalysts (d) is the standard anatase XRD.

film. All of the isotherms are in agreement with a typical type V. The pore distribution ranges from 2 nm to 15 nm, and the film mainly contains mesopores with diameters of 7.61, 7.27, 7.27, 7.61 and 8.78 nm for PEG 400, 800, 1000, 1500, and 2000, respectively. The pores are much larger than the organic molecules, which can provide access to the diffusion of dyes during the photodegradation reaction. The measurements manifest that the BET surface area of TiO_2 film is 31.36, 42.98, 47.72, 36.50 and 26.49 $m^2\ g^{-1}$ for PEG 400, 800, 1000, 1500, and 2000, respectively. It is clear that the film with PEG 1000 has the largest BET surface area of 47.72 $m^2\ g^{-1}$, which is quite beneficial for its application in a photodegradation reaction.

HRTEM and XRD measurements were performed on the powders under the same conditions as the films with percentage volume of TBOT of 15.15% and PEG 1000. Fig. 5a shows the presence of very small and nearly spherical nanoparticles of TiO_2 films. On average, these nanoparticles are about 10 nm in diameter. Fig. 5b clearly exhibits an interplanar spacing of 0.35 nm, a characteristic of the (101) plane in the anatase crystal of titania. The crystal phase of the catalysts was

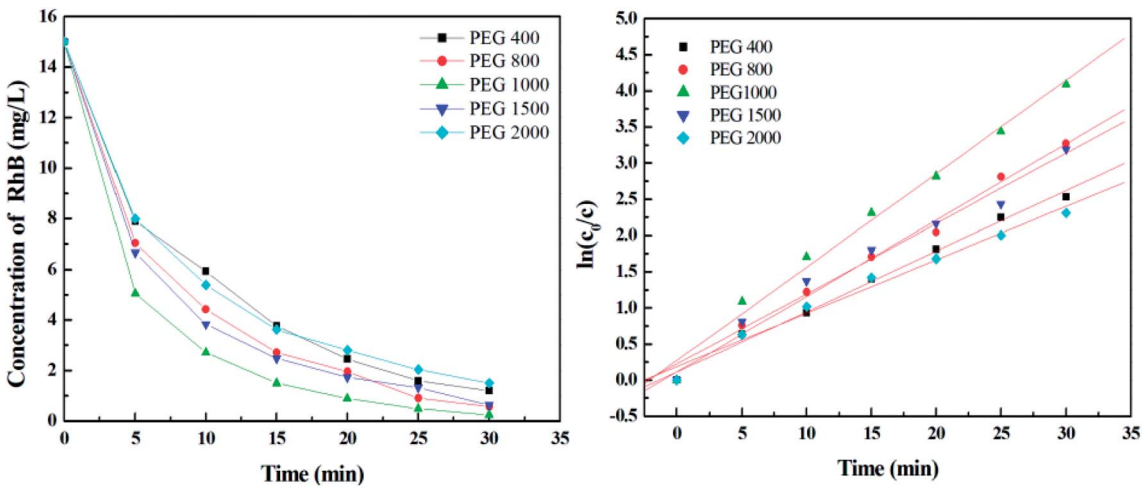

Fig. 6 Photodegradation of RhB under UV irradiation by TiO_2 films with PEG of different molecular weight.

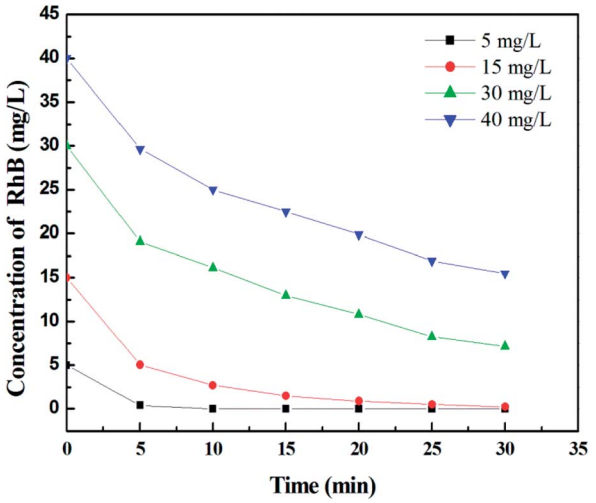

Fig. 7 Effect of initial RhB concentration on its photodegradation under UV irradiation. Initial concentrations: 5, 15, 30, and 40 mg L^{-1}.

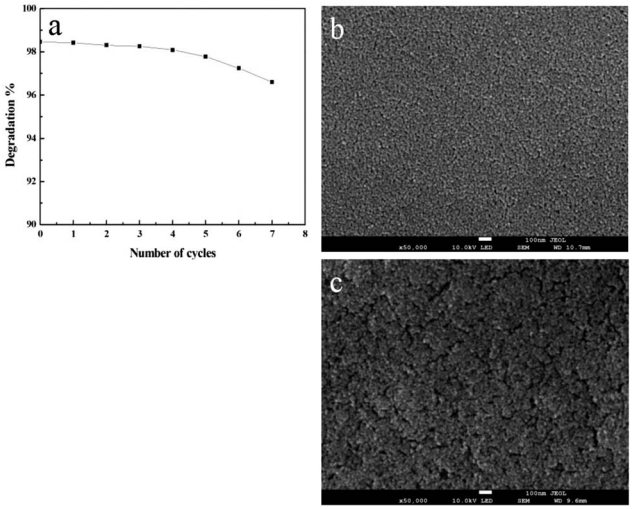

Fig. 8 (a) Degradation percentage degradation of RhB *versus* number of cycles. SEM images of films before (b) and after eight cycles (c) of photodegradation.

also characterized by XRD. As showed in Fig. 5c, sharp peaks at $2\theta = 25.4$, 37.6, 48.0, 53.9, and 55.1° are attributed to the (101), (004), (200), (105), and (211) planes, confirming the existence of anatase phase which is consistent with the spectral graph reported in the literature.[28]

3.2.2 Photodegradation of rhodamine B. To investigate the effect of specific surface area of TiO_2 films on dye photodegradation, experiments were carried out at the same conditions above. As calculated from Fig. 6, the optimal degradation efficiency is 98.33% in the absence of PEG 1000 and the photodegradation reaction rate constants are 0.0835, 0.1052, 0.1291, 0.0971 and 0.0738 min^{-1} for PEG 400, 800, 1000, 1500, and 2000, respectively. The results demonstrate that degradation efficiency increases with the molecular weight of PEG below 1000. However, when the PEG molecular weight is more than 1000, degradation efficiency decreases because of the reduction of the specific surface area.

3.3 Effect of initial rhodamine B concentration on its photodegradation

Fig. 7 shows the effect of initial RB concentration on its photodegradation for TiO_2 film with maximum thickness and specific surface area. It can be seen that as the RB concentration increases from 5 to 40 mg L^{-1} in 30 min, the degradation percentage decreases from 100% to 61.3%, suggesting that the concentration of dye should be controlled below 15 mg L^{-1} to remove the dye completely in a short time.

3.4 Catalyst reusability

Considering the catalyst cost, its reusability was investigated on TiO_2 film with maximum thickness and specific surface area. The catalyst was totally used eight times to see the efficiency in RB degradation. To compare the degradation efficiency, the degraded RB solution was removed and a fresh solution was injected into the same capillary after the last cycle of reaction. Degradation products were gathered at the end of each cycle. As revealed in Fig. 8, the degradation percentage in 30 minutes is 98.46% for the first time and 96.59% for the last time, demonstrating its stability after an eight time use.

3.5 Photodegradation mechanism of rhodamine B

TiO_2 films on capillary column was prepared by adding 15.15% of TBOT and calcining temperature of 500 °C and adding 1 g of PEG 1000 into the sol system. Degradation of 10 mg L^{-1} rhodamine B solution. The initial solution, the solution after degradation for 5 min and 30 min were analyzed by HPLC-MS, and the components of photodegradation products were analyzed. The photocatalytic degradation mechanism of rhodamine B by titania thin film catalyst was also studied.

Degradation intermediates of RB were recognized by positive ion mode mass spectra for products after 5 min and 30 min (Fig. 9). Mass peak at *m*/*z* 443 was observed for the initial solution, and is attributed to the RB molecule of a chloride ion. Peaks at *m*/*z* 415 and 387 is assigned to the deethylated intermediates of RB. The peak at *m*/*z* 318 originates from the intermediates of *m*/*z* 387 after losing a fragment of 74 mass units {(C2H5)2NH}. The product of *m*/*z* 274 due to the decarboxylation was also observed. Moreover, hydroxyl radical (·OH) attacks the double bond to cause a ring opening reaction. Peaks at *m*/*z* 143 and 152 are attributed to C9 compounds with an oxygen atom and C10 compounds with a nitrogen atom, respectively. For the mass spectra of products after 30 minutes, the signals of macromolecular intermediates were very weak. By contrast, signals at *m*/*z* 74 and 84 of unsaturated C6 compounds were relatively strong. These results suggest that RB was broken down into small molecules in 30 minutes, which were eventually decomposed into CO_2 and H_2O. A large number of experiments and mass spectrometry data proved that RB photodegradation was a process including gradual deethylation and breakage of the double bond in the benzene ring. The degradation mechanism is shown in Fig. 10.

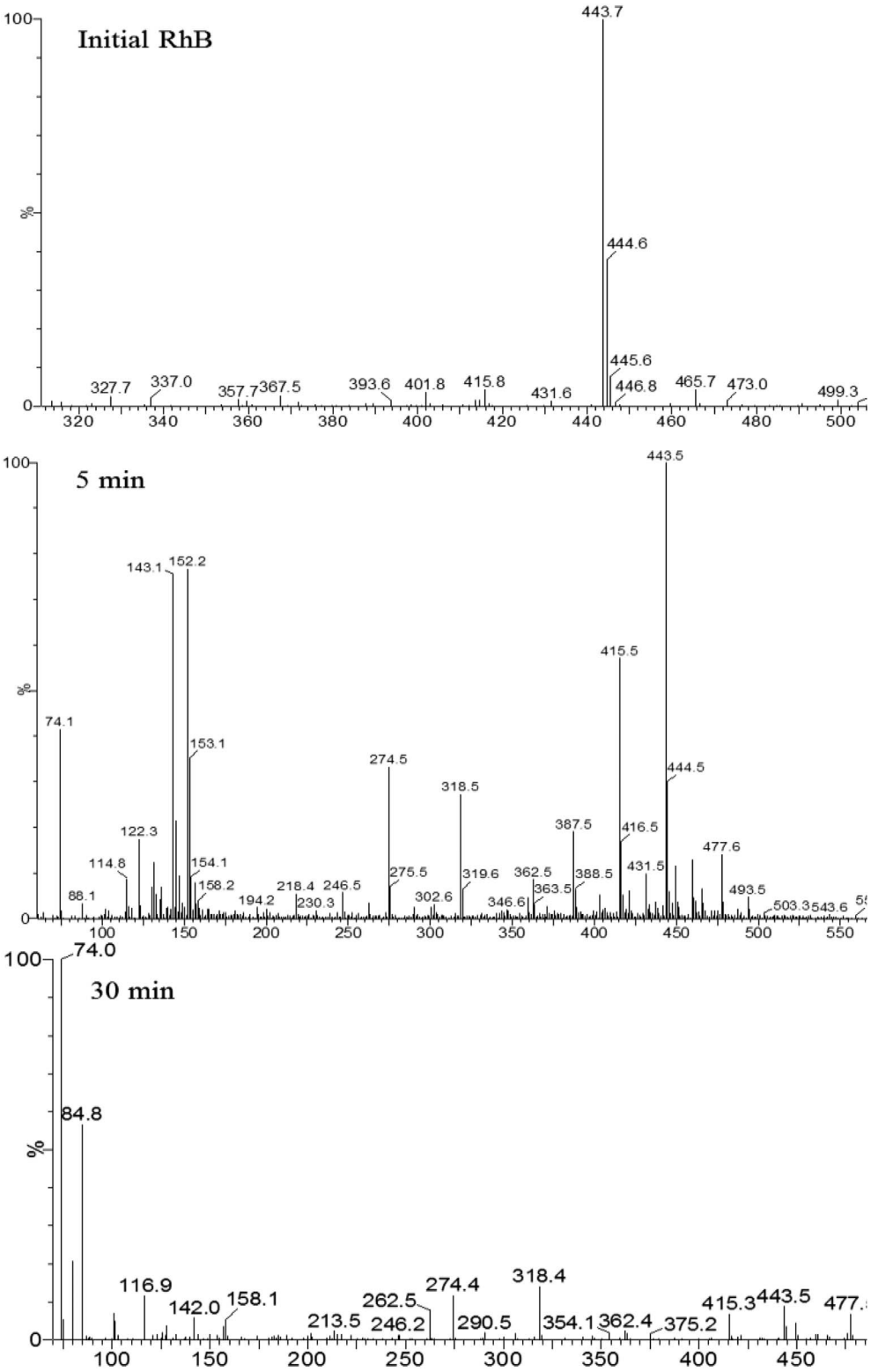

Fig. 9 Mass spectra of initial RhB solution and degradation products after 5 min and 30 min.

As shown in Fig. 11, the reaction was subjected to TOC analysis at the time of catalytic degradation. It can be seen that the concentration of TOC in the blank group was 2.049 mg L^{-1}, the concentration of TOC was 5.398 mg L^{-1} at the 0th minute when the reaction was not started, and the concentration of RB was decreased as the reaction progressed. After 30 minutes the TOC concentration of the solution was 3.353 mg L^{-1}. It means the RB was degradation efficiently by TiO_2 thin films. The TOC test results look same with the mass spectrometry analysis results.

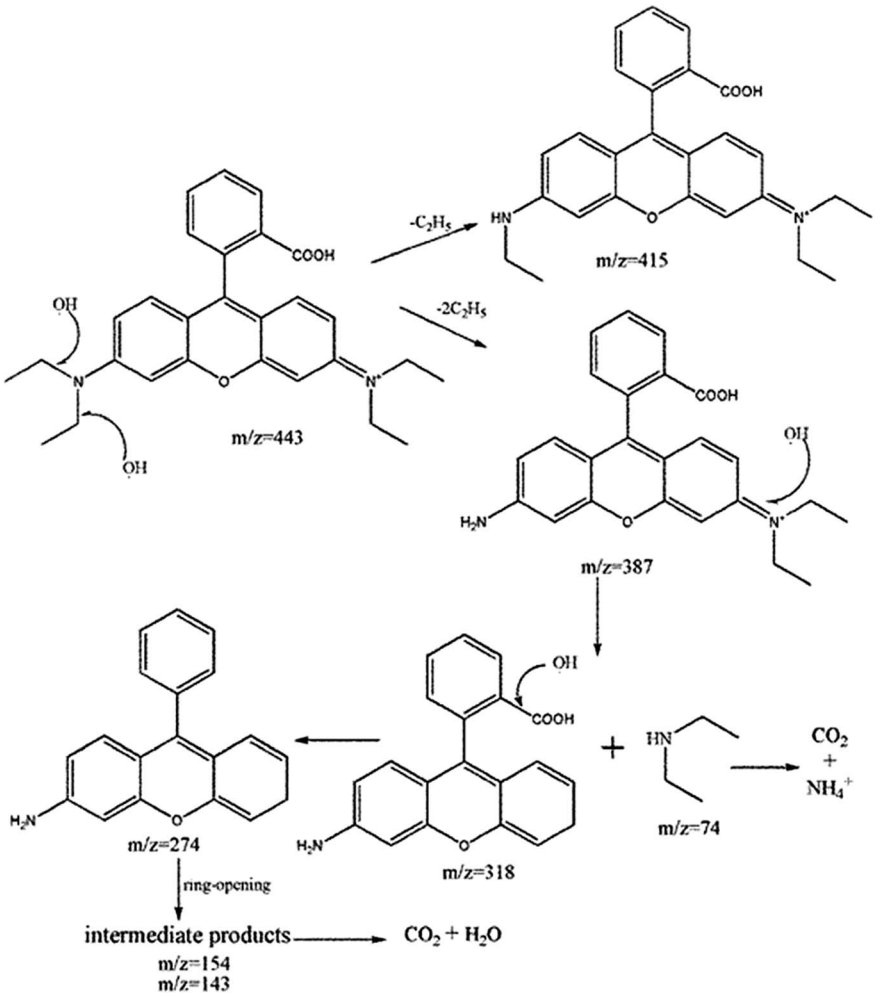

Fig. 10 Proposed degradation mechanism of RB.

	BLANK	0MIN	5MIN	10MIN	15MIN	20MIN	25MIN	30MIN
TOC	2.049mg/L	5.398mg/L	5.282mg/L	4.720mg/L	4.513mg/L	4.437mg/L	3.756mg/L	3.353mg/L

Fig. 11 TOC concentration of photocatalytic degradation of RB at 0–30 minutes with titanium dioxide.

4 Conclusions

In this paper, a certain thickness of TiO_2 film on capillary was fabricated using the sol–gel method for the first time. The prepared films possess a thickness of 361 nm and a good mesoporous structure with specific surface area of 47.72 $m^2 g^{-1}$ under the optimal synthesis conditions. The basic structure of the film is nearly spherical particles with a 10 nm diameters. With these merits, TiO_2 film exhibited superior photocatalytic performance when they were used as catalyst. Photodegradation experiments indicated that TiO_2 film catalyst could almost completely degrade RB of 15 mg L^{-1} in 30 minutes under UV irradiation. In addition, TiO_2 films are mechanically stable for repeated use to remove RB from wastewater, which is very significant in terms of cost savings and avoidance of secondary pollution. We believe that TiO_2 film catalysts may find application in the degradation of pollutants in the air.

Conflicts of interest

There are no conflicts to declare.

Acknowledgements

The authors would like to thank Analysis and Testing Center of Beijing University of Chemical Technology for all measurements.

References

1 C. S. Lan, W. N. Kai, S. Ibrahim, *et al.*, Preparation of Improved p-n Junction NiO/TiO_2 Nanotubes for Solar-Energy-Driven Light Photocatalysis, *Int. J. Photoenergy*, 2013, **2013**(1–2), 749–756.

2 J. Ryu and W. Choi, Substrate-Specific Photocatalytic Activities of TiO_2 and Multiactivity Test for Water Treatment Application, *J. Environ. Sci. Technol.*, 2008, **42**(1), 294.

3 N. Patel, R. Jaiswal, T. Warang, *et al.*, Efficient photocatalytic degradation of organic water pollutants using V–N-codoped TiO_2 thin films, *Appl. Catal., B*, 2014, **150–151**(1641), 74–81.

4 P. Péchy, T. Renouard, S. M. Zakeeruddin, *et al.*, Engineering of Efficient Panchromatic Sensitizers for Nanocrystalline TiO_2-Based Solar Cells, *J. Am. Chem. Soc.*, 2001, **123**(8), 1613–1624.

5 H. Klümper-Westkamp, S. Beling, A. Mehner, *et al.*, Semiconductor TiO_2 Gas Sensor for Controlling Nitrocarburizing Processes, *Met. Sci. Heat Treat.*, 2004, **46**(7), 305–309.

6 J. A. O. Méndez, C. R. López, E. P. Melián, *et al.*, Production of hydrogen by water photo-splitting over commercial and synthesised Au/TiO_2, catalysts, *Appl. Catal., B*, 2014, **147**(7), 439–452.

7 H. S. Kil, Y. J. Jung, J. I. Moon, *et al.*, Glycothermal Synthesis and Photocatalytic Properties of Highly Crystallized Anatase TiO_2 Nanoparticles, *J. Nanosci. Nanotechnol.*, 2015, **15**(8), 6193–6200.

8 S. Corvera and M. P. Czech, Synthesis and characterization of nitrogen-doped TiO_2 nanoparticles prepared by sol–gel method, *J. Sol-Gel Sci. Technol.*, 2012, **63**(1), 16–22.

9 M. Grandcolas, L. Yonge, O. V. Overschelde, *et al.*, Photocatalytic activity of TiO_2 nanodome thin films, *Ceram. Int.*, 2014, **40**(8), 12939–12946.

10 E. Blanco, J. M. Gonzálezleal and M. Ramírezdel Solar, Photocatalytic TiO_2 sol-gel thin films: Optical and morphological characterization, *Sol. Energy*, 2015, **122**(1), 11–23.

11 D. Nunes, A. Pimentel, J. V. Pinto, *et al.*, Photocatalytic behavior of TiO_2 films synthesized by microwave irradiation, *Catal. Today*, 2015, **278**, 262–270.

12 R. R. M. D. Sousa, F. O. D. Araújo, J. A. P. D. Costa, *et al.*, Deposition of TiO_2 Film on Duplex Stainless Steel Substrate Using the Cathodic Cage Plasma Technique, *Mater. Res.*, 2016, **19**(5), 1207–1212.

13 Y. Zhu, L. Zhang, L. Wang, *et al.*, The preparation and chemical structure of TiO_2 film photocatalysts supported on stainless steel substrates *via* the sol-gel method, *J. Mater. Chem.*, 2001, **11**(7), 1864–1868.

14 Q. Zhang and Z. Zhang, Preparation and Characterization of Nanocrystalline Fe-Doped TiO_2 Film on Different Substrates and Its Application in Degrading Dyeing Water, *J. Dispersion Sci. Technol.*, 2009, **30**(1), 110–114.

15 P. Kongsong, L. Sikong, S. Niyomwas, *et al.*, Enhanced Photocatalytic Degradation of Fulvic Acid Using N-Doped SnO_2/TiO_2 Thin Film Coated Glass Fibers under UV and Solar Light Irradiation for Drinking Water Purification, *Appl. Mech. Mater.*, 2016, **835**, 359–365.

16 T. H. Xie and J. Lin, Origin of Photocatalytic Deactivation of TiO_2 Film Coated on Ceramic Substrate, *J. Phys. Chem. C*, 2007, **111**, 9968–9974.

17 J. Krýsa, M. Baudys, M. Zlámal, *et al.*, Photocatalytic and photoelectrochemical properties of sol-gel TiO_2 films of controlled thickness and porosity, *Catal. Today*, 2014, **230**(230), 1554–1558.

18 D. Ljubas and L. Ćurković, Photocatalytic degradation of azo dyes by sol-gel TiO_2 films: effects of polyethylene glycol addition, reaction temperatures and irradiation wavelengths, *React. Kinet., Mech. Catal.*, 2015, **116**(2), 563–576.

19 S. T. Wang, M. Y. Wang, X. Su, *et al.*, Facile Preparation of SiO_2/TiO_2 Composite Monolithic Capillary Column and Its Application in Enrichment of Phosphopeptides, *J. Anal. Chem.*, 2012, **84**(18), 7763–7770.

20 J. M. Abi and J. Randon, Capillary monolithic titania column for miniaturized liquid chromatography and extraction of organo-phosphorous compounds, *Anal. Bioanal. Chem.*, 2011, **400**(5), 1241–1249.

21 M. H. Mangrola and V. G. Joshi, Synthesis and Characterization of Thin Films of Pure TiO_2 and Sr-Doped TiO_2 Prepared by Spin Coating Technique, *Int. J. Res. Advent Technol.*, 2014, **2**(1), 128–144.

22 D. N. Priya, J. M. Modak and A. M. Raichur, LbL fabricated poly(styrene sulfonate)/TiO_2 multilayer thin films for environmental applications, *ACS Appl. Mater. Interfaces*, 2009, **1**(11), 2684–2693.

23 L. Zhang, H. Liu, E. Zhao, *et al.*, Drying and nondrying layer-by-layer assembly for the fabrication of sodium silicate/TiO_2 nanoparticle composite films, *Langmuir*, 2011, **28**(3), 1816–1823.

24 G. Raúl, V. Mykola, R. Andrés, *et al.*, Surface Morphology of Heterogeneous Nanocrystalline Rutile/Amorphous Anatase TiO_2 Films Grown by Reactive Pulsed Magnetron Sputtering, *Plasma Processes Polym.*, 2010, **7**(9–10), 813–823.

25 S. Okunaka, H. Tokudome, Y. Hitomi, *et al.*, Facile preparation of stable aqueous titania sols for fabrication of highly active TiO_2 photocatalyst films, *J. Mater. Chem. A*, 2014, **3**(4): Advance Article.

26 S. T. Wang, M. Y. Wang, X. Su, *et al.*, Facile Preparation of SiO_2/TiO_2 Composite Monolithic Capillary Column and Its Application in Enrichment of Phosphopeptides, *J. Anal. Chem.*, 2012, **84**(18), 7763–7770.

27 L. X. Du, Z. T. Jiang and R. Li, Preparation of porous titania microspheres for HPLC packing by sol-gel method, *Mater. Lett.*, 2013, **95**(3), 17–20.

28 Y. Xie, X. Zhang, P. Ma, *et al.*, Hierarchical TiO_2 photocatalysts with a one-dimensional heterojunction for improved photocatalytic activities, *Nano Res.*, 2015, **8**(6), 2092–2101.